EURASIAN JOURNAL OF MATHEMATICAL AND COMPUTER APPLICATIONS
ISSN 2306–6172
Volume 13, Issue 4 (2025) 75– 84

NUMERICAL SIMULATION OF IMMERSED PLATE MOTION IN A CONVECTIVE LAYER UNDER RADIATION HEATING

Filimonov S. [1], **Gavrilov A.** , **Litvintsev K.**, **Vasiliev A.**, **Sukhanovskii A.**, **Frick P.**

Abstract We present the results of mathematical modeling of the motion of a plate immersed to a certain depth in the fluid and free-floating horizontally in a rectangular convective cell. The convective flow is provided by radiative heating at the bottom and cooling at the upper free boundary. It is shown that the character of the plate motion depends essentially on the optical properties of its surface. Three cases are considered: total transmission, absorption, and reflection of radiation. A good qualitative agreement is obtained between the results of the simulations performed and the experiments described in the literature.

Keywords: thermogravitational convection, immersed body, radiation heating.

AMS Mathematics Subject Classification: 76F35, 76F65, 80A21.

DOI: 10.32523/2306-6172-2025-13-4-75-84

1 Introduction

Thermogravitational convection determines the dynamics of various geophysical systems, such as the atmosphere, ocean, and mantle, and provides efficient transport of heat and various impurities [1]. The diversity of studies of convective flows is due to the fact that their formation and characteristics depend significantly on the intensity and direction of heating, geometric configuration, fluid properties, boundary and initial conditions [2, 3]. Convective systems with a free-floating body (or set of bodies) are of particular interest. The complex dynamics of such systems is determined by the mutual influence of the floating body and convective flow. The floating body blocks heat [4] and momentum transfer and changes the flow structure, while the flow under the action of viscous stresses moves the body. Studies of the dynamics of free-floating bodies and their influence on the structure of convective flows are carried out both experimentally [5, 6, 7, 8] and numerically [9, 10].

Usually, in simulations, the heat source is defined either in the form of boundary conditions of the first kind (fixed temperature at the boundaries of the simulation domain) or in the form of boundary conditions of the second kind (fixed heat flux at the boundaries of the simulation domain). In real systems (atmosphere, ocean) the main source of convective flows is solar radiation. Convective flows are provided by heating of the Earth's surface and oceans, which determine the characteristics of the atmosphere both on the global scale [11, 12, 13, 14] and locally [15, 16, 17, 18]. Cloud clusters can have a great influence on the formation of convective flows and

[1]Corresponding Author.

total heat transfer. To understand the basic mechanisms determining the dynamics of the convective system in the presence of large objects influencing the distribution of radiation and motion of the fluid, studies in simple model formulations are required.

Radiation heats the underlying surface, providing in the free layer conditions close to those of the second kind, but has an important feature related to the non-uniformity of heat flux distribution over the surface. The non-uniformity is associated with the re-reflection of incident radiation from stationary objects, which creates a complex but stationary profile of heat flux distribution, and with moving bodies, which either completely or partially shade the underlying surface. In addition, the solid body itself can absorb radiation and be a source of convective flow.

A laboratory experiment on studying the dynamics of a free-floating immersed body in a convective layer with radiation heating is described in [19], in which the motions of bodies with different optical properties, namely, the motions of submerged disks reflecting, absorbing, or transmitting radiation, were studied. In this paper we reproduce these experiments numerically, since numerical simulations allow us not only to follow the dynamics of a floating body, but also to obtain a complete picture of the heat and mass transfer in such a complex system.

2 Mathematical model

The numerical simulation of turbulent convection in a rectangular cavity with a free-floating heat-insulating body inside the fluid volume is realized in the software package SigmaFlow [20]. The system of equations describing the convective flow of a Newtonian incompressible fluid in the Boussinesq approximation has the following form:

$$\begin{aligned} \frac{\partial \mathbf{u}}{\partial t} + (\mathbf{u}\cdot\nabla)\,\mathbf{u} &= -\frac{\nabla p}{\rho_0} + \nu\nabla^2\mathbf{u} - \mathbf{g}\beta(T-T_0) \\ \frac{\partial T}{\partial t} + (\mathbf{u}\cdot\nabla)\,T &= \chi\nabla^2 T \\ \nabla\cdot\mathbf{u} &= 0, \end{aligned}$$

where $\mathbf{u}$ is velocity; ρ_0 is density, T is temperature; T_0 is volume-averaged temperature, p is pressure, $\mathbf{g}$ is free-fall acceleration, ν is kinematic viscosity, χ is diffusivity, and β is coefficient of thermal expansion.

The motion of the insulating body is described by Newton's equation. The impact of the body against the walls is considered inelastic. The simulations of the body motion in the fluid is done using the immersed boundary method [21]. The numerical schemes used have second-order accuracy in both space and time. A center-difference scheme of second order in spatial step is used to approximate the convective and diffusion terms, and a Crank-Nicholson scheme of second order in time is used to build the algorithm for the unsteady solution. The optimal spatial resolution is chosen based on the results of [10]. A detailed description of the mathematical model and the results of its validation are presented in [22].

At all boundaries of the cell Γ_s the no-slip boundary conditions are applied

$$\mathbf{u}|_{\Gamma_s} = 0.$$

At the boundary of a free-floating body Γ_b, the velocity of the fluid is equal to plate velocity u_{plate}, which was found from the solution of Newton's equation,

$$\mathbf{u}|_{\Gamma_b} = \mathbf{u}_{plate}.$$

The side walls of the cell and the body were considered adiabatic

$$\left.\frac{\partial T}{\partial n}\right|_{\Gamma_s} = \left.\frac{\partial T}{\partial n}\right|_{\Gamma_b} = 0,$$

and at the lower and upper boundary of the computational domain, the temperature was set to

$$T|_{y=0} = T_h, \qquad T|_{y=H} = T_c.$$

At the initial moment of time, the temperature of the liquid and the plate was set equal to $T_0 = 298.15K$, the velocity of the liquid was set equal to zero, and the plate was located at the center of the cell with respect to the x-axis.

All simulations with and without a free-floating body were performed for a fixed Prandtl number $\mathrm{Pr} = \nu/\chi = 7$.

The distribution of the incident radiation flux was calculated on the basis of the finite-volume method [23]. To simulate the radiation source in the form of an LED strip [19], a uniform radiation flux in the solid angle π, which corresponds to the angle of light propagation 120^o, was set. The condition of partial transmission and partial mirror reflection of radiation was used for the side walls of the cell, and the condition of complete absorption was used for the lower boundary.

3 Statement of the problem

The motion of a solid plate in a rectangular cell filled with water is simulated. The dimensions of the cell and the plate are shown in Fig. 1. The properties of the liquid are summarized in Tab. 1. The floating body density $\rho = 1200\,\mathrm{kg/m^3}$, its heat capacity $C_p = 1300\,\mathrm{J/(kg^*K)}$, and the thermal conductivity $\lambda = 0.38\,\mathrm{W/(m^*K)}$. The problem is solved in a pseudo-two-dimensional formulation, the depth of partitioning in the transverse direction is 1 cell (depth 10 mm), symmetry conditions are set on the end walls for all values. The grid step in the solution plane is 0.25 mm. The time step is 0.03 s. The simulation time is 8000 s. The float has one degree of freedom, along the x-axis. The bottom wall is made as a plate of textolite, whose thermophysical properties coincide with those of the plate. On the upper cells of the computational domain associated with the textolite, the distribution of the heat flux was set, simulating the radiation heating of the lower surface of the convective cell. The average value of the incident radiation flux was 308 $\mathrm{W/m^2}$. The heat transfer from the textolite to the liquid was modeled using the coupled heat transfer method. The heat flux distribution profile over the surface of the textolite was obtained by preliminary calculation of the radiation flux (see Fig. 2). Adiabatic conditions were set at the lower boundary of

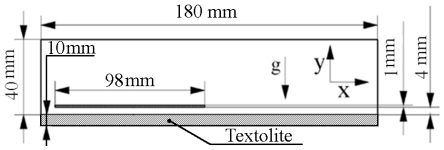

Figure 1: Schematic diagram of the computational domain

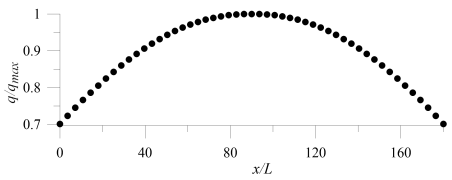

Figure 2: Normalized radiation heat flux at the bottom of the cell

Table 1: Thermophysical properties of water

Density	$\rho = 998.15$ kg/m^3
Dynamic viscosity	$\mu = 0.001$ Pa· s
Thermal conductivity	$\lambda = 0.598$ W/(m · K)
Heat capacity	$C_p = 4183$ J/(kg · K)
Thermal expansion coefficient	$\beta = 0.000211$ 1/K

the computational domain. A uniform heat flux equal to -308 W/m^2 minus the heat reflected by the float was set on the upper wall. Three cases of the plate were considered: mirror-reflecting, transparent, and radiation absorbing. For the second and third cases, the radiative heat flux under the plate was set equal to zero, i.e., the plate created a shadow.

4 Results

4.1 Case 1. Mirror-reflecting plate

In the first case considered, the plate has a mirror top surface and the radiation falling on it is reflected, while a shadow is formed on the textolite below it. Fig. 3 shows the dynamics of temperature and velocity magnitude in the cell at different moments of time after the beginning of simulations. It can be seen that at the initial moment of time there is heating of the surface of the textolite outside the plate. At the same time, due to the shape of the incident heat flux near the plate, the temperature of the textolite is slightly higher than at the edges of the cell. As a consequence, powerful symmetric vortices develop at the edges of the plate, which become more complex with time: the number of vortical structures grows and they fill the area above the plate, but remain symmetric. At some point in time, two symmetric vortices formed at different ends of the plate interact (see Fig. 3d). The symmetry is broken and the plate goes into motion.

When the plate reaches the wall, a strong upwelling flow is generated in the other, open part of the cell, which forms a large vortex above the plate (Fig. 4). This vortex pulls the plate away from the wall and moves it in the opposite direction. When it reaches the opposite wall the whole process is repeated. Thus, the plate oscillates from wall to wall with an average period of about 390 s. Fig. 5 shows the dynamics of the plate's center.

4.2 Case 2. Transparent plate

In the second case, the plate is transparent to radiation and the radiation flux completely falls on the textolite. The shape of the temperature distribution on the surface follows the profile of the incident radiation flux (see Fig. 2). The amount of heat entering the system is larger than in the first case, so the temperature difference in the cell grows faster and the flow forms and begins to move the plate sooner (see Fig. 6).

For some time the plate, as in the first case, makes periodic oscillations from wall to wall. However, as the textolite plate warms up, the motion slows down and the plate stops at one of the walls (Fig. 8). The temperature and velocity fields after the

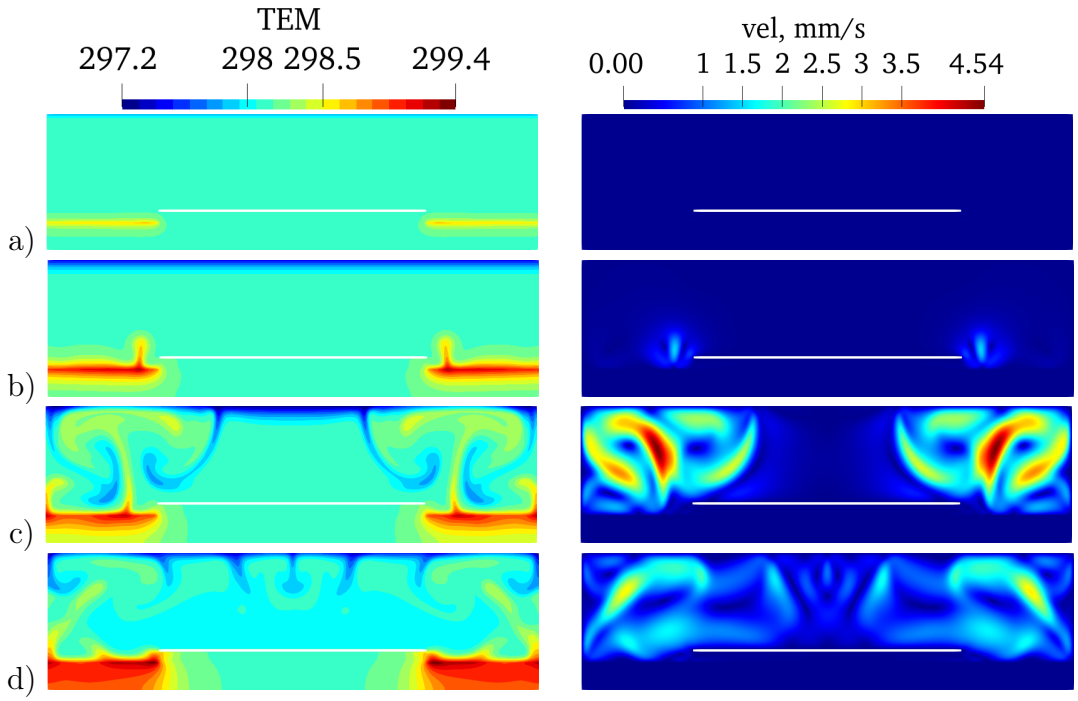

Figure 3: Temperature and velocity magnitude in the cell at different time moments after the start of simulations: 12 s (a), 60 s (b), 102 s (c), and 300 s (d). Case 1

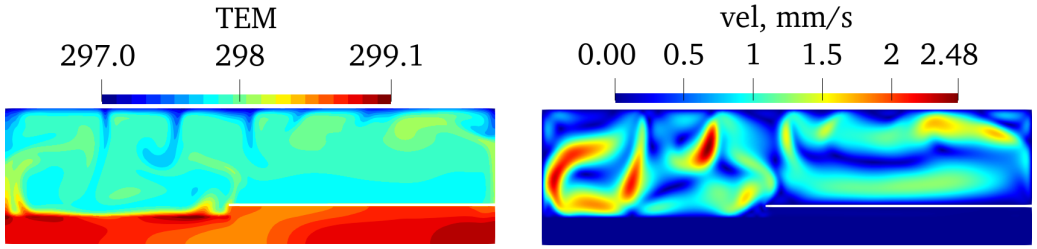

Figure 4: Temperature and velocity magnitude distribution in the cell before plate detachment from the wall. Case 1

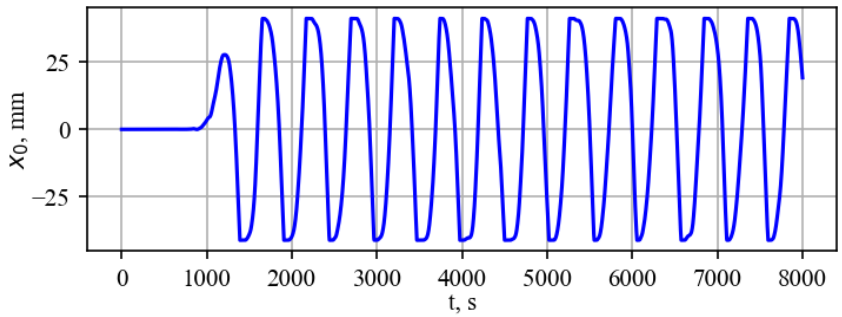

Figure 5: Displacements of the plate center. Case 1

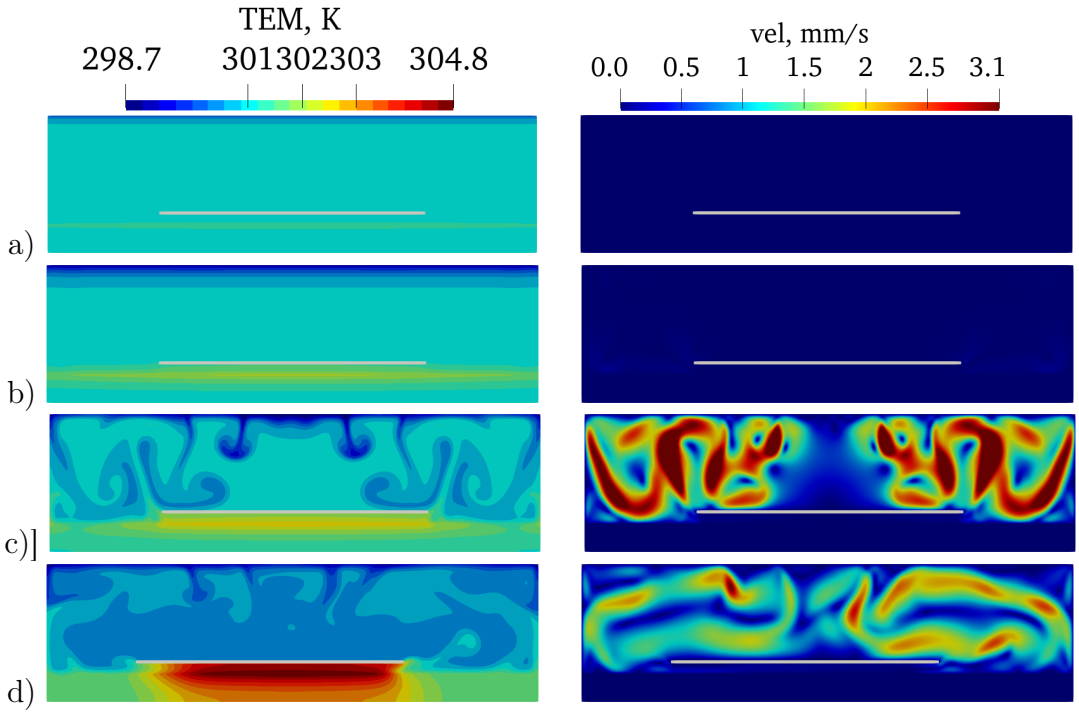

Figure 6: Temperature and velocity magnitude in the cell at different time moments after the start of simulations: 12s (a), 60 s (b), 102 s (c), and 300 s (d). Case 2

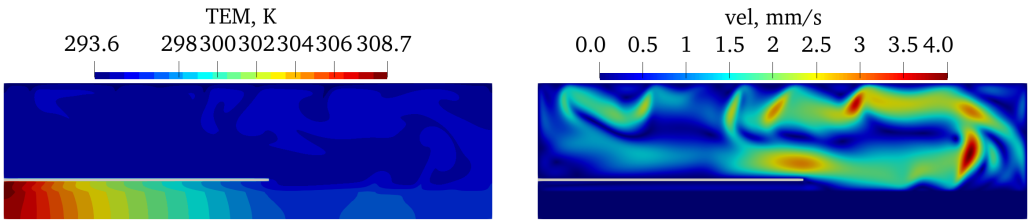

Figure 7: Temperature and velocity magnitude distribution in the cell when the plate is locked near the wall. Case 2

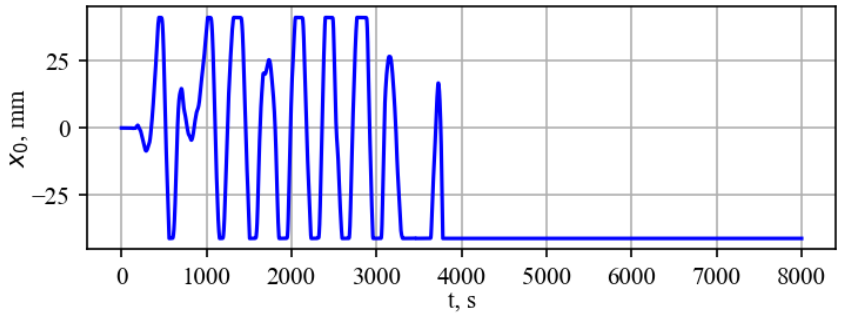

Figure 8: Displacements of the plate center. Case 2

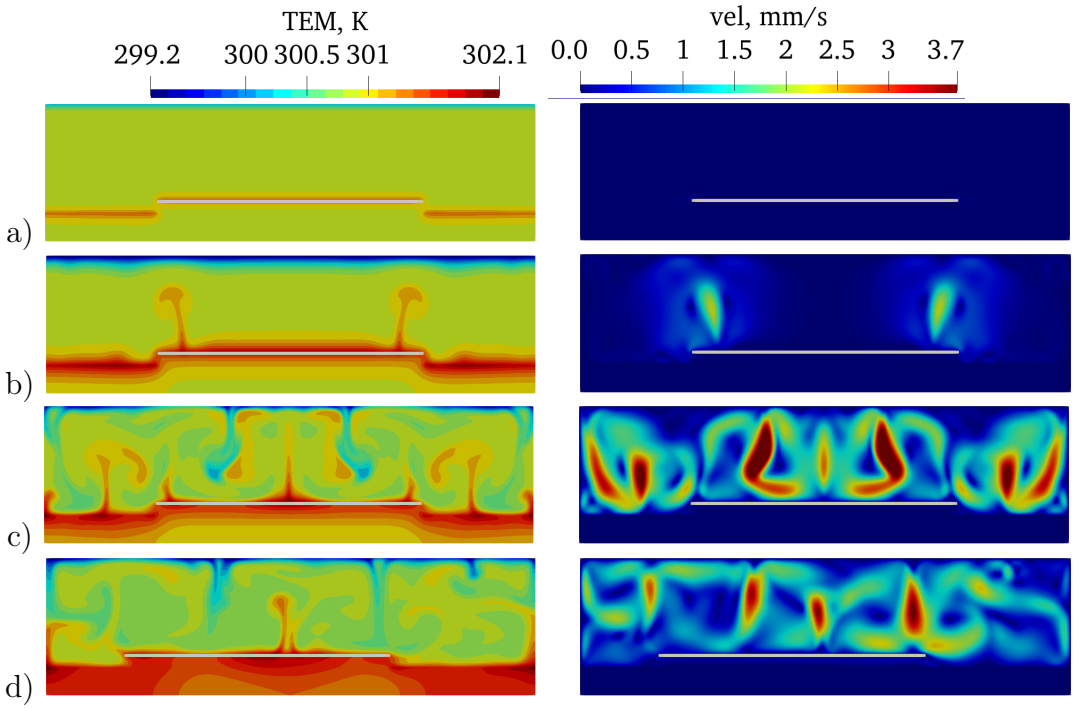

Figure 9: Temperature and velocity magnitude in the cell at different time moments after the start of simulations: 12 s (a), 60 s (b), 102 s (c), and 300 s (d). Case 3

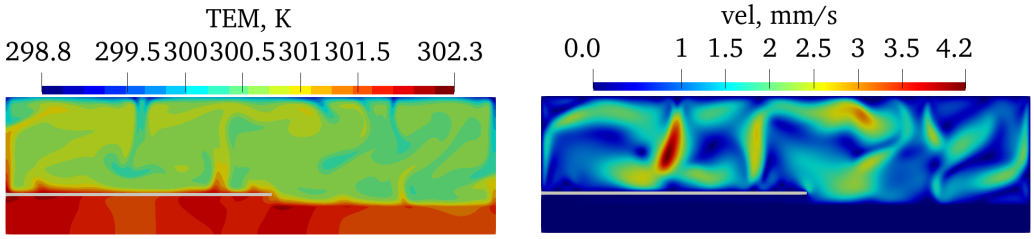

Figure 10: Temperature and velocity magnitude distribution in the cell when the plate is locked near the wall. Case 3

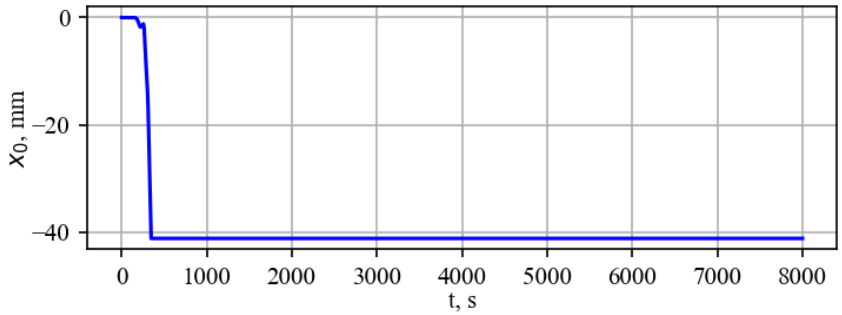

Figure 11: Displacements of the plate center. Case 3

plate stops at the wall are shown in Fig. 7 and indicate the formation of a vortex that pushes the plate against the wall.

4.3 Case 3. Absorbing plate

In the third case, the plate completely absorbs the radiation falling on it. Then, the textolite under the plate remains in the shadow and is not heated. As can be seen from the heating dynamics, the first noticeable convective flows are formed near the plate boundaries, where the maximal horizontal temperature gradients occur (see Fig. 9,b). Since convective vortices arise above the plate (and not at the periphery), they begin to interact earlier than in the previous cases. At the 300th second, the plate relative to the center, but the first approach of the plate to the wall ends with its capture by the vortex, which pushes it against the wall. (see Fig. 9d)).

Fig. 10 shows the temperature and velocity magnitude field after the plate stops at the wall. It can be seen that the heated liquid rises from the plate along the cell wall. This leads to the formation of a vortex, which on the one hand pushes the plate against the wall and on the other hand prevents the formation of a large vortex like the one shown in the Fig. 7. The plate is locked at the wall and does not move further (Fig. 11).

Summary

We have performed numerical modeling of the dynamics of an immersed plate in a closed cell heated by radiation. Numerical simulations reproduce the character of motion of plates with different optical properties established in the experiments [19]. As in the experiment, the plate covered with reflective material makes periodic oscillations from wall to wall. In the other two cases, the plate stops at one of the walls, but its locking mechanism is different. In the case of a transparent plate, it first behaves like a mirror plate, and as it warms up it comes to a state where it cannot break away from the wall, due to the flow formed under it. The light-absorbing plate stops at the wall at the first touch due to the formation of a strong vortex above the plate. The Tab. 2 shows for comparison the average vertical temperature differences obtained for each case in the experiment and the simulations (it should be taken into account that in the experiment there are only estimates of the heat flux).

In case 1, in which periodic oscillations are carried out, we can quantitatively compare the characteristics of the plate motion. It turns out that the period of complete oscillation in the experiment is significantly longer (1700 seconds vs. 390 seconds), but the difference is mainly due to the significantly longer duration of standing of the

Table 2: Mean temperature difference between the upper and lower boundaries ΔT and Rayleigh number. Experimental data from the paper [19]

Case	$\Delta T_{exp}, K$	Ra_{exp}	$\Delta T_{calc}, K$	Ra_{calc}
Reflecting	0.8	$8.9 \cdot 10^5$	1.6	$1.8 \cdot 10^6$
Transparent	1.1	$1.1 \cdot 10^6$	5.3	$5.8 \cdot 10^6$
Absorbing	1	$1 \cdot 10^6$	2.2	$2.4 \cdot 10^6$

plate at the wall, not to the velocity of its motion. If we calculate the average speed of motion without taking into account the standing time, it turns out that the speed of motion in the simulation is only one-third higher than in the experiment (0.9 mm/s vs. 0.6 mm/s). When comparing the simulation results with the experimental results, it should be kept in mind that in the experiments the plate was made in the form of a circular disk, and the simulations were performed in a two-dimensional formulation, which actually assumes a rectangular shape of the plate and does not take into account the three-dimensional structure of the emerging convective flows.

Acknowledgement

The study was done under the RSF project 22-61-00098. The development of a mathematical model of radiation transfer was carried out under state contract with IT SB RAS (124062400029-2).

References

[1] Golitsyn G. S., *Natural processes and phenomena: Waves, planets, convection, climate, and statistics*, Moscow, Fizmatlit, 2004. (in Russian)

[2] Gershuni G. Z., Zhukhovitskii E. M., *Convective instability of incompressible fluids*, Keter Publishing House, 1976.

[3] Getling A. V, *Rayleigh-Bénard convection. Structure and dynamics*, Moscow, Editorial URSS, 1999. (in Russian)

[4] Vasiliev, A. Y., Sukhanovskii, A. N., Frick, P. G., *Influence of horizontal heat-insulating plates on the structure of convective flows and heat transfer in a closed cavity*, Computational Continuum Mechanics, Vol. 15, no. 1 (2023), P.83-97.

[5] Zhang J., Libchaber A., *Periodic boundary motion in thermal turbulence*, Physical Review Letters, Vol. 84, no. 19 (2000), P.4361-4364.

[6] Zhong J.-Q., Zhang J., *Dynamical states of a mobile heat blanket on a thermally convecting fluid*, Physical Review E, Vol. 75, no. 5 (2007), P.055301.

[7] Popova E. N., Frik P. G., *Large-scale flows in a turbulent convective layer with an immersed moving thermal insulator*, Fluid Dynamics, Vol. 38 (2003), P.862-867.

[8] Frick P., Popova E., Sukhanovskii A., and Vasiliev A., *A random 2D walk of a submerged free-floating disc in a convective layer*, Physica D Nonlinear Phenomena, Vol. 455 (2023), P.133882.

[9] Mao Y., Zhong J. Q., Zhang J. T., *The dynamics of an insulating plate over a thermally convecting fluid and its implication for continent movement over convective mantle*, Journal of Fluid Mechanics, Vol. 868 (2019), P.286-315.

[10] Frick P., Filimonov S., Gavrilov A., Popova E., Sukhanovskii A., Vasiliev A., *Rayleigh-Bénard convection with immersed floating body*, Journal of Fluid Mechanics, Vol. 979 (2024), P.A23.

[11] Harlander U., Sukhanovskii A., Abide S., Borcia I. D., Popova E., Rodda C., Vasiliev A., Vincze M., *New laboratory experiments to study the large-scale circulation and climate dynamics*, Atmosphere, Vol. 14, no. 5 (2023), P.836.

[12] Sukhanovskii A., Popova E., Vasiliev A., *A shallow layer laboratory model of large-scale atmospheric circulation*, Geophysical & Astrophysical Fluid Dynamics, Vol. 117, no. 3 (2023), P.155-176.

[13] Vasiliev A. Y., Popova E. N., Sukhanovskii A. N., *The flow structure in a laboratory model of atmospheric general circulation*, Computational Continuum Mechanics, Vol. 16, no. 2 (2023), P.321-330. (In Russian)

[14] Sukhanovskii A., Gavrilov A., Popova E., Vasiliev A., *The study of the impact of polar warming on global atmospheric circulation and mid-latitude baroclinic waves using a laboratory analog*, Weather and Climate Dynamics, Vol. 5, no. 2 (2024), P.863-880.

[15] Litvintsev K. Yu., Dekterev A. A., Meshkova V. D., Filimonov S. A., *Influence of radiation on the formation of wind and temperature regimes in urban environment*, Thermophysics and Aeromechanics, Vol. 30 (2024), P.683-694.
[16] Meshkova V., Dekterev A., Litvintsev K., Filimonov S., *Current approaches to studying the level of pedestrian comfort in urban development*, E3S Web Conferences, Vol. 435 (2023), P.05004.
[17] Bykov A. V., Vetrov A. L., Frick P. G., Sukhanovskii A. N., Kalinin N. A., Stepanov R. A., *Numerical modeling of extreme conditions of planetary atmosphere*, Geographical bulletin, Vol. 4, no. 67 (2023), P.85-98. (In Russian)
[18] Bykov A. V., Vetrov A. L., Kalinin N. A., *Severe heat forecasting in Krasnoyarsk using the WRF-ARW regional model*, Hydrometeorological Research and Forecasting, Vol. 382, no. 2 (2024), P.65-85. (in Russian)
[19] Vasiliev A. Y., Popova E. N., Frick P. G., Sukhanovskii A. N., *Drift of a Free-floating Body in a Convective Layer Heated by Radiation*, Journal of Siberian Federal University. Mathematics & Physics, Vol. 16, no. 5 (2023), P.562-571.
[20] Dekterev A. A., Gavrilov A. A., Minakov A. A., *New features of SigmaFlow code for thermo-physical problems solving*, Modern Science: research, ideas, results, technologies, Vol. 30 (2024), P.117-122. (in Russian)
[21] Mittal R., Iaccarino G., *Immersed boundary method*, Annual Review of Fluid Mechanics, Vol. 37 (2005), P.239-261.
[22] Filimonov S. A., Gavrilov A. A., Dekterev, A. A., Litvintsev, K. Y., *Mathematical modeling of the interaction of a thermal convective flow and a moving body*, Computational Continuum Mechanics, Vol. 16, no. 1 (2023), P.89-100. (in Russian)
[23] Litvintsev K., Sentyabov A., *Application of the finite volume method for calculating radiation heat transfer in applied problems*, Bulletin of the South Ural State University. Ser. Mathematical Modelling, Programming & Computer Software, Vol. 14, no. 3 (2021), P.77-91.

S. Filimonov,
Kutateladze Institute of Thermophysics SB RAS,
1, Lavrentiev avenue, 630090, Novosibirsk,
Russia,
Email: bdk@inbox.ru,

A. Gavrilov,
Kutateladze Institute of Thermophysics SB RAS,
1, Lavrentiev avenue, 630090, Novosibirsk,
Russia,

K. Litvintsev,
Kutateladze Institute of Thermophysics SB RAS,
1, Lavrentiev avenue, 630090, Novosibirsk,
Russia,

A. Vasiliev,
Institute of Continuous Media Mechanics,
1, Academika Koroleva st, 614018, Perm,
Russia,

A. Sukhanovskii,
Institute of Continuous Media Mechanics,
1, Academika Koroleva st, 614018, Perm,
Russia,

P. Frick,
Institute of Continuous Media Mechanics,
1, Academika Koroleva st, 614018, Perm,
Russia.

Received 18.10.2024, Accepted 08.12.2024, Available online 31.12.2025.